Z. Phys. D 39, 41–48 (1997)

ZEITSCHRIFT
FÜR PHYSIK D

A comparative study on the spin asymmetry and integrated cross sections for the electron-impact ionization of atomic hydrogen

J. Berakdar[1], P.F. O'Mahony[2], F. Mota-Furtado[2]

[1] Atomic and Molecular Physics Laboratories, Research School of Physical Sciences and Engineering, Australian National University, Canberra, ACT 0200, Australia (Tel. + 61-6/249 2453, Fax: + 61-6/249 2452)
[2] Department of Mathematics, Royal Holloway, University of London, Egham, Surrey TW20 OEX, UK

Received: 19 May 1996 / Final version: 19 September 1996

Abstract. The spin asymmetry and integrated spin-unresolved cross sections for the electron-impact ionization of atomic hydrogen are studied. The influence of individual final-state interactions on these quantities is elucidated by investigating the collision process within the plane-wave impulse approximation, the first Born approximation and within an independent Coulomb particle model. The predictions of the latter approximation for the shape and magnitude of the spin asymmetry are in good agreement with experimental data over the entire measured energy range. The effects of final-state electronic correlations are investigated by the inclusion of the electronic Coulomb density-of-states factor as well as by employing a three-body Coulomb wave-function for the description of the final state. For ionization of hydrogen-like ions the calculated asymmetry parameter has a positive slope near threshold indicating that such an energy dependence is due to the electron-nucleus interactions. At threshold the results are analyzed in light of the Wannier theory of threshold ionization.

PACS: 34.80.Dp

I Introduction

Electron-impact ionization of atomic hydrogen is the simplest process leading to three continuum charged particles. Hence, this reaction provides an ideal testing ground for theoretical models treating the motion of Coulomb particles in the continuum. Full information on this collision process is obtained by measuring the ionization rate for given vector momenta and spin states of the two escaping electrons. Various integrated cross sections test different aspects of the ionization dynamics. For example, it has been shown by Wannier [1] that at threshold the analytical dependence of the total ionization cross section on the total excess energy derives from the phase-space volume available for double escape. Ever since an immense amount of experimental and classical, semi-classical and quantum mechanical theoretical investigations (see e.g. [1–13]) have been carried out to test the Wannier prediction of the slope of the total cross section. The original Wannier theory assumes ${}^1S^e$-states only for the outgoing electrons. Thus, the Wannier theory provides no estimate of the spin states occupied by the electrons in the final channel. A measure of the relative magnitudes of singlet to triplet scattering is given by the spin asymmetry A [14–17]. Upon extension of the Wannier treatment to arbitrary L, S and π (total angular momentum, total spin and parity) [6, 18], it has been concluded that all L-states have the same energy dependence at threshold and nearly all $LS\pi$-states (in particular singlet and triplet states) possess the same threshold law. These findings allow one to conclude that A does not depend on the excess energy near threshold although an exact value of A is not provided. Recently, however, an inspection of near threshold experimental data for the spin asymmetry revealed a slightly positive slope for A with increasing excess energy [19]. This behaviour has not been confirmed by recent calculations using the hidden crossing theory [13], which show a considerable variation of A near threshold. It has been suggested [13] that this variation is due to anharmonic corrections to the Wannier threshold law for triplet spin states.

The analysis of the above mentioned theories is restricted to the threshold region. To describe the entire energy region the problem has recently been treated fully numerically by using the convergent close-coupling technique (CCC) [20]. Excellent agreement with the experimental data for the spin asymmetry and total cross section has been achieved although the threshold region (down to 1.4 eV above threshold was reached) could not be included in the treatment due to the rapidly increasing number of pseudo states needed to reach convergence. In addition to the above mentioned theories there are a number of other theoretical approaches which have been compared with experiment in [14].

The aim of this work is to systematically investigate over a wide energy region the influence of various interactions involved in the ionization process on the spin non-resolved integrated cross sections and the spin

asymmetry and to relate properties of these quantities with each other. To this end we start with a very simple theoretical model for the final-state description in which the escaping electrons occupy plane waves, namely the plane wave impulse approximation (PWIA). Then we investigate the influence of the distortion of the motion of one electron due to the nuclear field by employing the first Born approximation (FBA) according to which the ionized electron occupies a target continuum state. Further, we study the reaction in a model of independent Coulomb particles (2C) in which the escaping electrons move independently in the Coulomb field of the nucleus. To study the influence of final-state electronic correlations we investigate a model in which the final-state wavefunction provided by the 2C model is multiplied by the final-state electronic density-of-state factor, this model is called hereafter (CDS2C). This procedure has proved to be, to some extent, capable of describing the angular distribution of the final state products [21–23]. In addition, we investigate the case where the final state is represented by a product of three Coulomb waves (therefore we refer to this model as 3C), each of which describes the individual three two-body subsystems [24, 25]. Finally, to illustrate the influence of the nuclear field we briefly present spin asymmetry results for an increased nuclear charge, i.e. for ionization of hydrogen-like ions. It is shown that, without resorting to elaborate numerical methods, the spin asymmetry can be satisfactorily described in shape and magnitude by the 2C model over the entire energy region. The CDS2C and 3C theories show similar behaviour as the CDS2C model results from the 3C theory in the case where the radial part of the interelectronic Coulomb wave is neglected. When employing the 3C and CDS2C methods, the results for the spin asymmetry and the energy distribution between the two-electrons are quite poor near threshold. In contrast, the spin asymmetry is reasonably well described in shape and magnitude within the 2C model and is found to vary very slowly at threshold in agreement with predictions based on the Wannier theory. With increasing nuclear charge the spin asymmetry shows a positive slope near threshold as a function of the excess energy indicating that this effect is due to electron-nucleus interactions. Atomic units are used throughout.

II Theoretical models

The total cross section for the electron-impact ionization of the hydrogen atom in its ground state is given by

$$\sigma(E) = \frac{(2\pi)^4}{v_i} \int |T(\mathbf{k}_a, \mathbf{k}_b)|^2 \delta(E - E_i)\, \mathrm{d}^3 k_a \mathrm{d}^3 k_b. \tag{1}$$

In (1) E_i, v_i are respectively the total energy in the initial channel and the velocity of the incoming projectile with respect to the nucleus. The total energy in the final channel, denoted by E in (1), is given by

$$E = \frac{k_a^2}{2} + \frac{k_b^2}{2}. \tag{2}$$

where $\mathbf{k}_a, \mathbf{k}_b$ are the momenta of the outgoing electrons with respect to the nucleus, which is assumed to be infinitely heavy with respect to the electron mass. The transition-matrix element appearing in (1) has the form

$$T(\mathbf{k}_a, \mathbf{k}_b) = \langle \Psi | W_i | \Phi \rangle \tag{3}$$

where W_i refers to the perturbation operator in the initial channel. The state of the three-body system in the initial channel is described by $|\Phi\rangle$ whereas $|\Psi^-\rangle$ represents the three particle Coulomb system above the complete fragmentation threshold. In the following we choose $|\Phi\rangle$ to have the form

$$\langle \mathbf{r}_a, \mathbf{r}_b | \Phi \rangle = (2\pi)^{-3/2} \exp(i\mathbf{k}_i \cdot \mathbf{r}_a) \varphi(\mathbf{r}_b) \tag{4}$$

where $\mathbf{r}_a, \mathbf{r}_b$ are the position vectors (with respect to the nucleus) of the incoming projectile and the initially bound electron, respectively and $\varphi(\mathbf{r}_b)$ is the bound state wavefunction. The operator W_i then becomes

$$W_i = \frac{1}{|\mathbf{r}_a - \mathbf{r}_b|} + \frac{-1}{r_a}. \tag{5}$$

In the 2C approximation the electron-electron final-state interaction is neglected which results in the approximate final-state wavefunction

$$\begin{aligned} \langle \mathbf{r}_a, \mathbf{r}_b | \Psi^- \rangle \approx \Psi_{2C}(\mathbf{r}_a, \mathbf{r}_b) &= (2\pi)^{-3} \exp(i\mathbf{r}_a \cdot \mathbf{k}_a + i\mathbf{r}_b \cdot \mathbf{k}_b) \\ &\times \mathrm{N}_a\, {}_1F_1\left[i\frac{Z_a}{k_a}, 1, -i(k_a r_a + \mathbf{k}_a \cdot \mathbf{r}_a) \right] \\ &\times N_b\, {}_1F_1\left[i\frac{Z_b}{k_b}, 1, -i(k_b r_b + \mathbf{k}_b \cdot \mathbf{r}_b) \right] \end{aligned} \tag{6}$$

where $Z_a = -Z = Z_b$ are the electron-nucleus product charges and Z is the charge of the residual nucleus. The normalization constants N_j; $j = a, b$ are given by

$$N_j = \exp\left(-\frac{\pi Z_j}{2k_j} \right) \Gamma\left(1 - i\frac{Z_j}{k_j} \right); \quad j = a,\ b. \tag{7}$$

The final-state wavefunctions in the FBA and PWIA models derive from the expression (6) in the case $Z_a \equiv 0$, $Z_b = -Z$ and $Z_a \equiv 0 \equiv Z_b$, respectively. According to [24, 25], the inclusion of final-state interelectronic correlations results in the 3C-wavefunction

$$\begin{aligned} \Psi_{3C}(\mathbf{r}_a, \mathbf{r}_b) = N_{ab}\, {}_1F_1\left[i\frac{1}{2k_{ab}}, 1, -i(k_{ab} r_{ab} + \mathbf{k}_{ab} \cdot \mathbf{r}_{ab}) \right] \\ \times \Psi_{2C}(\mathbf{r}_a, \mathbf{r}_b) \end{aligned} \tag{8}$$

where N_{ab} is given by (7), $\mathbf{r}_{ab} = \mathbf{r}_a - \mathbf{r}_b$ and $\mathbf{k}_{ab} = (\mathbf{k}_a - \mathbf{k}_b)/2$ are the interelectronic relative coordinate and its conjugate momentum, respectively. A simpler way to account for the final-state interaction of the escaping electrons has been proposed in [21–23]. In this case the wavefunction $\Psi_{2C}(\mathbf{r}_a, \mathbf{r}_b)$ is multiplied by the Coulomb density-of-state factor N_{ab}, i.e.

$$\Psi_{CDS2C}(\mathbf{r}_a, \mathbf{r}_b) = N_{ab} \Psi_{2C}(\mathbf{r}_a, \mathbf{r}_b) \tag{9}$$

It should be noted here that final-state wavefunctions due to PWIA, FBA, 2C and 3C models are normalized to delta

functions in momentum space whereas the function, given by (9) is not normalized and hence does not conserve flux.

III Results and discussion

A Total cross sections and excess-energy distributions

Based on a classical stability analysis of the motion of two escaping electrons in the field of a nucleus of charge Z, Wannier [1] derives the energy-functional dependence of the total cross section (1) at vanishingly small excess energy E to be

$$\sigma(E) \propto E^{\mu/2-1/4}, \tag{10}$$

where the Wannier index μ is given by

$$\mu = \frac{1}{2}\sqrt{\frac{100Z-9}{4Z-1}}. \tag{11}$$

The threshold behaviour of $\sigma(E)$, derived from the quantum mechanical expression (1), is controlled by the low-energy limit of the final state wavefunction (6) since, at threshold, the initial binding energy of the system (13.6 eV) is much larger than the excess energy at which threshold ionization is considered. The threshold behaviour of the wavefunction Ψ_{2C} is readily deduced by employing the following parametrization of k_a and k_b

$$K := (k_a^2 + k_b^2)/2 = E, \ \tan\beta = \frac{k_a}{k_b} \tag{12}$$

in which case the wavefunction (6) can be expanded in terms of Bessel functions, $J_0[x]$, at small K [26, 27]. The leading order term in E reads

$$\lim_{E\to 0} \Psi_{2C}(\mathbf{r}_a, \mathbf{r}_b) = (2\pi)^{-3} N_a N_b \chi(\mathbf{r}_a, \mathbf{r}_b \hat{\mathbf{k}}_a, \hat{\mathbf{k}}_b) \tag{13}$$

where

$$\chi = J_0\left[2\sqrt{-Z_a(r_a + \hat{\mathbf{k}}\cdot\mathbf{r}_a)}\right] J_0\left[2\sqrt{-Z_b(r_b + \hat{\mathbf{k}}_b\cdot\mathbf{r}_b)}\right]. \tag{14}$$

For the evaluation of the cross section (1) the absolute values of the normalization constants N_j; $j = a, b$ are decisive. From (7) it is clear that

$$\lim_{Z_j\to 0} N_j \to 1, \quad j = a, b, ab. \tag{15}$$

Further, near threshold the functions N_j; $j = a, b$ cast in terms of the parametrization (12) become

$$|N_j|^2 = -2\pi\frac{Z_j}{k_j}; \quad j = a, b \tag{16}$$

or

$$|N_a|^2 = \frac{1}{\sqrt{E}}\frac{-2\pi Z_a}{\sqrt{2}\sin\beta}, \tag{17}$$

$$|N_b|^2 = \frac{1}{\sqrt{E}}\frac{-2\pi Z_b}{\sqrt{2}\cos\beta}. \tag{18}$$

Near to threshold the Ψ_{3C} wavefunction can be expanded as [28]

$$\lim_{E\to 0} \Psi_{3C}(\mathbf{r}_a, \mathbf{r}_b) = (2\pi)^{-3} N_a N_b N_{ab} \chi(\mathbf{r}_a, \mathbf{r}_b, \hat{\mathbf{k}}_a, \hat{\mathbf{k}}_b) \times I_0[\sqrt{2(r_{ab} + \hat{\mathbf{k}}\cdot\mathbf{r}_{ab})}] \tag{19}$$

where $I_0(x)$ is a modified Bessel function. For large arguments x the function $I_0(x)$ is unbound. Hence, the normalization N_{ab} corresponding to this function must vanish at threshold. In fact, near threshold N_{ab} exhibits the behaviour

$$|N_{ab}|^2 = \frac{2\pi}{\sqrt{Ef(\Theta_k, \beta)}} \exp\left[\frac{-2\pi}{\sqrt{2Ef(\Theta_k, \beta)}}\right], \tag{20}$$

where $f(\Theta_k, \beta) = \sqrt{1 - \sin 2\beta\cos\Theta_k}$ and the angle Θ_k is defined as $\cos\Theta_k := \hat{\mathbf{k}}_a\cdot\hat{\mathbf{k}}_b$. From (20) it is readily concluded that $|N_{ab}|^2$ decreases, basically, exponentially with decreasing excess energies. This behaviour is at variance with experimental findings and the Wannier theory predictions [1].

To investigate the behaviour of integrated cross sections, (1) is reformulated in the coordinates (12) and the integral over K is readily performed to give

$$\sigma(E) = \frac{(2\pi)^{-2}}{v_i} E^2 \int \sin^2 2\beta |T|^2 \mathrm{d}\beta\, \mathrm{d}^2\hat{\mathbf{k}}_a\, \mathrm{d}^2\hat{\mathbf{k}}_b. \tag{21}$$

To take advantage of the overall rotational invariance of the system we introduce, with respect to an arbitrary set of axes, the azimuthal angles φ_a, φ_b of the vectors $\hat{\mathbf{k}}_a, \hat{\mathbf{k}}_b$ respectively. To separately investigate the effects of the spatial part of the wavefunction and its normalization $N := N_a N_b N_{ab}$ we define the reduced matrix element $T_r := T/N$. The expression (21) has then the form

$$\sigma(E) = \frac{(2\pi)^{-2}}{v_i} 2E^2 \int \sin^2 2\beta |N|^2 |T_r|^2 \mathrm{d}\beta\, \mathrm{d}\cos\Theta_k \mathrm{d}\varphi_a \mathrm{d}\varphi_b. \tag{22}$$

From (13) we conclude that at threshold the reduced matrix element T is reduced in the PWIA, FBA and 2C approximations to $T_r(\hat{\mathbf{k}}_a, \hat{\mathbf{k}}_b) = \langle\chi|W_i|\Phi\rangle$ which depends only upon $\hat{\mathbf{k}}_a, \hat{\mathbf{k}}_b$. Thus, for $E \ll 1$ the expression (22) simplifies to

$$\sigma(E) = g\, E \int_0^E \sin 2\beta |N|^2 \mathrm{d}E_a. \tag{23}$$

In (23) we transformed the integral over β to an integral over the energy E_a of one of the electrons and introduced the factor

$$g := \frac{(2\pi)^{-2}}{v_i} 2\int |T_r|^2 \mathrm{d}\cos\Theta_k \mathrm{d}\varphi_a \mathrm{d}_b. \tag{24}$$

Wannier [1] (see also [5]) showed that an independent Coulomb particle model (2C) yields a total cross section σ which is linearly dependent on the excess energy E. This is readily verified from (17, 18) where in the 2C model the relation $|N|^{-2} = |N_a N_b|^{-2} \propto E\sin 2\beta$ holds and from (23)

it follows then that $\sigma(E) \propto E$. In addition, we conclude from (23) that in the 2C approximation the excess energy E is equally shared between the two escaping electrons, i.e. $d\sigma(E, E_a)/dE_a = constant$ which is in accordance with the conclusions of [5]. The absolute value of this constant is determined by g, i.e. by the momentum-space angular correlations of the electrons since the behaviour of g is controlled by $T_r(\hat{\mathbf{k}}_a, \hat{\mathbf{k}}_b)$. Thus, it is expected that the absolute value of the cross section is poorly described since in the 2C model the angular correlations between the electrons are neglected (compare [29]).

In a PWIA treatment the normalization factor reduces to $|N|^2 = 1$ (compare Eq. 15). From (22) it follows then that $\sigma(E) \propto E^2$ [30] and for the excess-energy distribution we deduce $\mathrm{d}\sigma(E, \beta)/\mathrm{d}\beta = \sin^2 2\beta$ which means that the equal-energy sharing between the two electrons is the most probable according to the PWIA. From (15) we deduce that in the FBA the normalization constant is given by $N = N_b$. From (18, 23) it is obvious that $\sigma(E) \propto E^{1.5}$ and for the excess-energy sharing we obtain $\mathrm{d}\sigma(E, E_a)/\mathrm{d}E_a = \sqrt{E_a}$. The latter distribution is not symmetric with respect to $E_a = E - E_a$. This is due to the fact that in the FBA the two electrons are not treated on an equal footing. Thus, upon employing an antisymmetrized wavefunction the FBA model results in an oscillating cross section for $\mathrm{d}\sigma(E, E_a)/\mathrm{d}E_a$.

The case of 3C and CDS2C theories is much more involved since for these models the separation, given by (23, 24), is not applicable. As pointed out in the preceding, near to threshold, the absolute magnitude of cross sections calculated within the CDS2C and 3C models is expected to be determined by the factor given by (20). In fact it has been analytically shown in [30] that when the final-state wavefunction provided by the PWIA is multiplied by the factor (20) the total cross section $\sigma(E)$ behaves as $\sigma(E) \propto E^{5/4} \exp(-\pi/\sqrt{E})$. Similar considerations [31] lead to the conclusion that the total cross section in the CDS2C model possess the behaviour $\sigma(E) \propto E^{1/4} \exp(-\pi/\sqrt{E})$. At lower excess energies, the predictions of the CDS2C and 3C models for the energy distribution between the two outgoing electrons depend strongly on the behaviour of $|N_{ab}|^2$. To explicitly show this the factor $|N_{ab}|^2$ is depicted in Fig. 1a and b for lower ($E = 1$ eV) and intermediate ($E = 50$ eV) excess energies, respectively. From Fig. 1a it is evident that $|N_{ab}|^2$ is sharply peaked around an angular configuration in which the two electrons are emitted opposite to each other. In this angular configuration the energy distribution is strongly peaked around equal energy sharing. This behaviour is directly reflected in the corresponding cross sections, as will be shown below. As the excess energy increases the electron-electron repulsion dominates only in a limited region around the configuration where the two electrons recede from the nucleus with equal vector velocities. Thus allowing for further structures in $|N_{ab}|^2(\Theta_k, \beta)$ to emerge. However, these structures have only a minor influence on the cross section as in this case the magnitude of $|N_{ab}|^2$ tends to unity and the radial part $T_r = T/N$ of the transition amplitude becomes decisive.

To verify the above predictions and the range of validity of the expansion (13) the cross sections, as given by (1), are directly calculated within the 2C, FBA, PWIA, 3C and CDS2C models by using the wavefunctions given by (6, 8, 9). The results are shown in Fig. 2a, b. The energy-sharing distribution is constant within the 2C model and the magnitude of $\sigma(E)$ is given by the surface below the solid curve in Fig. 2a. As shown in [29] the absolute value of $\sigma(E)$ is overestimated by the 2C-model implying that the electronic angular correlations are incorrectly described by this approach. Therefore, the magnitude of $\mathrm{d}\sigma(E, E_a)/\mathrm{d}E_a$ is also overestimated by the 2C approach. A non-antisymmetrized FBA-wavefunction results in an excess energy-distribution described by $\mathrm{d}\sigma(E, E_a)/\mathrm{d}E_a = \sqrt{E_a}$ whereas antisymmetrization leads to considerable variation in the energy distribution. We remark here that the Wannier treatment supported by experimental evidence [3, 11, 32] indicates a basically flat energy distribution at threshold. In contrast, the CDS2C and 3C models predict a sharply peaked energy distribution around equal-energy sharing of the outgoing electrons. This behaviour is directly connected to that shown in

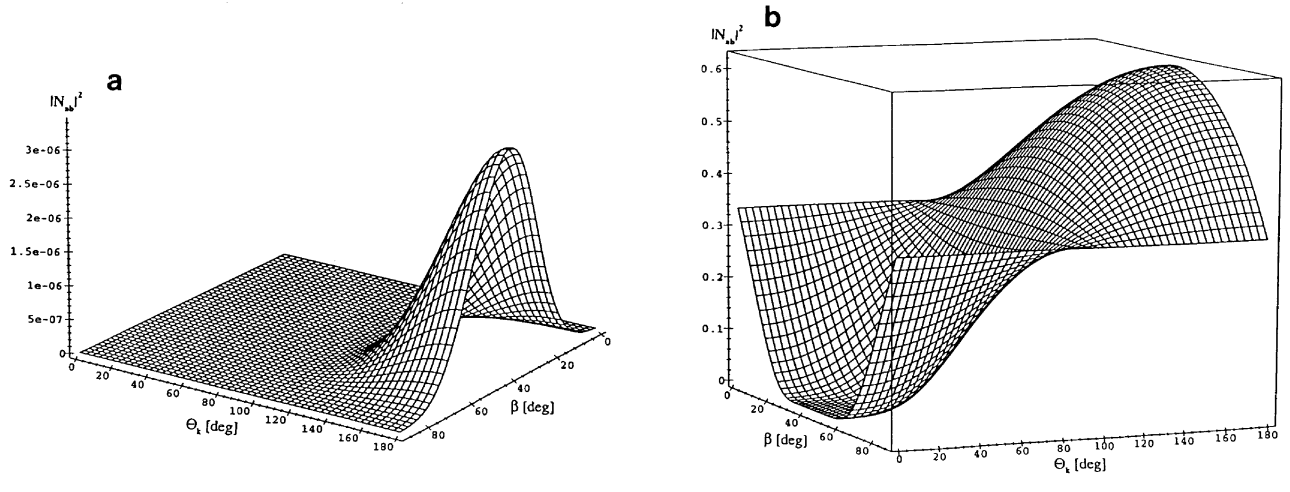

Fig. 1a, b. The Coulomb density-of-states $|N_{ab}|^2(\Theta_k, \beta)$, as defined by (20), is depicted as function of Θ_k and β. The excess energy is chosen as $E = 1$ eV **a** and $E = 50$ eV **b**

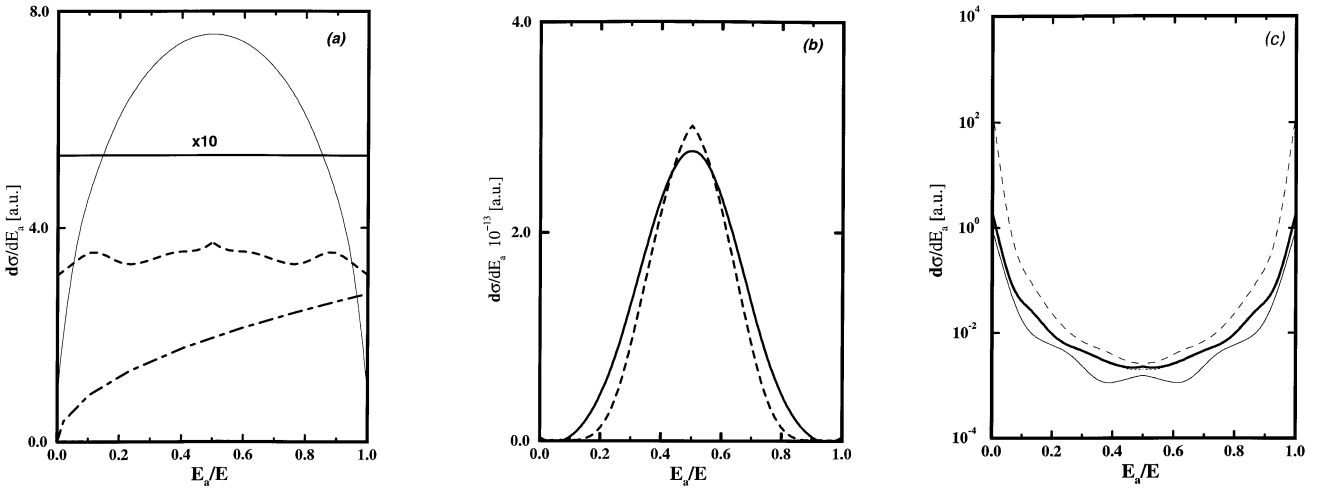

Fig. 2a–c. The spin non-resolved singly differential cross section $d\sigma/dE_a$ for the electron-impact ionization of atomic hydrogen as function of E_a/E where E_a is the energy of one of the ejected electron and $E = 80$ meV is the excess energy. In **a** the *solid curve* represents the results of the 2C approximation scaled down by a factor of 10 whereas the PWIA results are denoted by the *solid light curve*. The PWIA results have been multiplied by a factor of 80. The FBA yields the results shown by the *dashed curve* whereas the *dashed-dotted curve* are the results of the FBA without taking into account the indistinguishibility of the two continuum electrons. In **b** the results of the 3C (*solid curve*) and CDS2C (*dashed curve*) models are shown. The CDS2C results have been multiplied by a factor of 4×10^{10}. **c** shows $d\sigma/dE_a$ versus (E_a/E) at an incident energy of 500 eV ($E = 486.4$ eV). The FBA (*dotted*) and 2C (*solid curve*) results coincide with each other. The PWIA results are denoted by the dashed curve whereas the *solid light curve* refers to the results of the CDS2C method

Fig. 1a. Interestingly, the magnitude of the cross section $d\sigma(E, E_a)/dE_a$ calculated within the 3C model is several order of magnitude bigger than that provided by the CDS2C model. This is due to the diverging behaviour of the radial part of (19). However, transition amplitudes are still convergent when using the 3C method due to convergent factors provided by the transition operator, given by (5), and the initial-state wavefunction.

At higher excess energies (Fig. 2c) results of the FBA and the 2C theories for $d\sigma(E, E_a)/dE_a$ are identical and agree in shape with the prediction of the CDS2C and PWIA models. According to these approximations the most probable energy distribution is an asymmetric one which indicates that the dominating ionization mechanism is a direct collision process in which the projectile hits the atomic electron at large impact parameter losing only little of its initial momentum. Due to the indistinguishability of the two final state electrons $d\sigma(E, E_a)/dE_a$ must be symmetric with respect to $E_a = E/2$.

B Spin asymmetry

There is an indication that at threshold the factorization of the total cross section in the form (23) is of general validity [12] and not only pertinent to the approximations used here. In fact, for the Wannier theory such a factorization (23) can be deduced from the prediction that the $d\sigma(E, \beta)/ d\beta$ is a flat function of β. As pointed out in the preceding discussion, (23) leads to the conclusion that the momentum-space angular correlations which are described by the quantity g, are irrelevant for the functional forms of $\sigma(E)$ and $d\sigma(E, \beta)/d\beta$. However, the absolute value of $\sigma(E)$ is determined by g. A way of testing for the structure of the quantity g rather than its absolute value is provided by comparing with the spin asymmetry A. The spin asymmetry A is a measure of the spin states occupied by the continuum electrons and is defined as

$$A(E) := \frac{\sigma^s(E) - \sigma^t(E)}{\sigma^s(E) + 3\sigma^t(E)} \tag{25}$$

where σ^s and σ^t are the total ionization cross sections for singlet and triplet scattering, respectively, and are given by

$$\sigma^{s,t}(E) = \frac{(2\pi^4)}{v_i} \int |T^{s,t}|^2 \delta(E - E_i) d^3k_a d^3k_b \tag{26}$$

where the singlet and triplet T-matrices are given by

$$T^s = [1 + \mathscr{A}_{ab}]\, T(\mathbf{k}_a, \mathbf{k}_b)$$
$$T^t = [1 - \mathscr{A}_{ab}]\, T(\mathbf{k}_a, \mathbf{k}_b). \tag{27}$$

In (27) the exchange T-matrix has been introduced

$$\mathscr{A}_{ab} T(\mathbf{k}_a, \mathbf{k}_b) = T(\mathbf{k}_b, \mathbf{k}_a). \tag{28}$$

The spin-unresolved cross sections (integrated and fully differential) are statistical averages of triplet and singlet scattering cross sections, i.e.

$$\frac{d^6\sigma(E)}{d^3\mathbf{k}_a d^3\mathbf{k}_b} = \frac{1}{4}\frac{d^6\sigma^s(E)}{d^3\mathbf{k}_a d^3\mathbf{k}_b} + \frac{3}{4}\frac{d^6\sigma^t(E)}{d^3\mathbf{k}_a d^3\mathbf{k}_b}. \tag{29}$$

The important point now is that in any adequate description of threshold ionization the two low-energy electrons should be treated on an equal basis. As a result the normalization factor N should have the property $N(\mathbf{k}_a, \mathbf{k}_b) = N(\mathbf{k}_b, \mathbf{k}_a)$ (this is not the case in the FBA). Provided the threshold factorization (23) is valid, this

yields for the spin asymmetry

$$A(E) := \frac{g^s - g^t}{g^s + 3g^t} \tag{30}$$

where g^s, g^t are the functions introduced in (24) and calculated with T^s and T^t, respectively. Equation (30) is not valid for the CDS2C and 3C models since at threshold the factorization (23) is not applicable in case of these approximations.

Two important conclusions can be immediately deduced from (30): *a*) The spin asymmetry is a feature of the spatial part of wavefunctions and does not depend on its normalization. Further A tests for the momentum-space angular correlations. *b*) As pointed out in the preceding section $g^{s/t}$ are excess-energy independent at threshold. Thus, the spin asymmetry should not depend upon the excess energy in the energy region close to threshold. The last conclusion has been also drawn in [18] where the Wannier threshold theory has been employed to predict that all L-states have the same energy dependence at threshold and nearly all $LS\pi$-states (in particular singlet and triplet states) possess the same threshold law which leads to a constant A at threshold. It is worth noting that the Wannier-theory prediction of a constant A can be combined with the general factorization (23) to deduce that, in general, the quantities g^s and g^t possess the same analytical (weak) excess-energy dependence. The Wannier theory of threshold ionization provides, however, no estimate of the absolute value of A since $g^{s/t}$ are not directly evaluated.

In the present work A is calculated according to (26, 25). In Fig. 3a the results for the spin asymmetry are depicted. As mentioned above, the momentum-space angular correlation factors $g^{s/t}$ are poorly described by the 2C treatment which results in a too large absolute value of the total cross section [29]. Thus, according to (30) it is justified to believe that the 2C treatment would be inadequate in describing the behaviour of A. Surprisingly, the spin asymmetry measurements are well reproduced by the 2C theory over the entire measured energy region. At first glance this appears to be in contradiction with the conclusions of the preceding section. We remark, however, that the spin asymmetry A involves a ratio of the quantities g^s and g^t. This leads to the conclusion that g^s and g^t contain a common angular factor which is wrongly described by the 2C approximation but which cancels out when taking the ratio of g^s to g^t (otherwise the absolute value of the total cross section should be reproduced by the 2C model [29]). The measurements shown in Fig. 3a, b indicate that ionization into the singlet channel dominates that into the triplet channel. Using the PWIA it can be shown analytically [30] that, at threshold, ionization into the triplet channel is prohibited. This is remarkable in so far as within the PWIA the total potential is assumed to be short range which results in a plane-wave description of the outgoing electrons. This leads to the speculation that the value of A is pertinent to the long-range behaviour of the Coulomb interaction. The FBA description fails to account for the behaviour of the spin asymmetry, as evident from Fig. 3a, b. This is mainly due to the fact that the two escaping electrons are not treated on equal footing, thus, $N(\mathbf{k}_a, \mathbf{k}_b) \neq N(\mathbf{k}_b, \mathbf{k}_a)$. Hence, (30) is not valid within the FBA. At this stage it is interesting to note that an equal treatment of the two escaping electrons is not a guarantee for an adequate description of A. This is most clearly seen by considering the spin asymmetry in the CDS2C and 3C models. In this case the emerging electrons are treated symmetrically and the normalization constants have the property $N(\mathbf{k}_a, \mathbf{k}_b) \neq N(\mathbf{k}_b, \mathbf{k}_a)$. However, the factorization, given by (23), is not valid in this case since the normalization N depends on $\hat{\mathbf{k}}_a, \hat{\mathbf{k}}_b$. As evident from Fig. 3a, b the CDS2C and the 3C models are not capable of describing the threshold behaviour of the

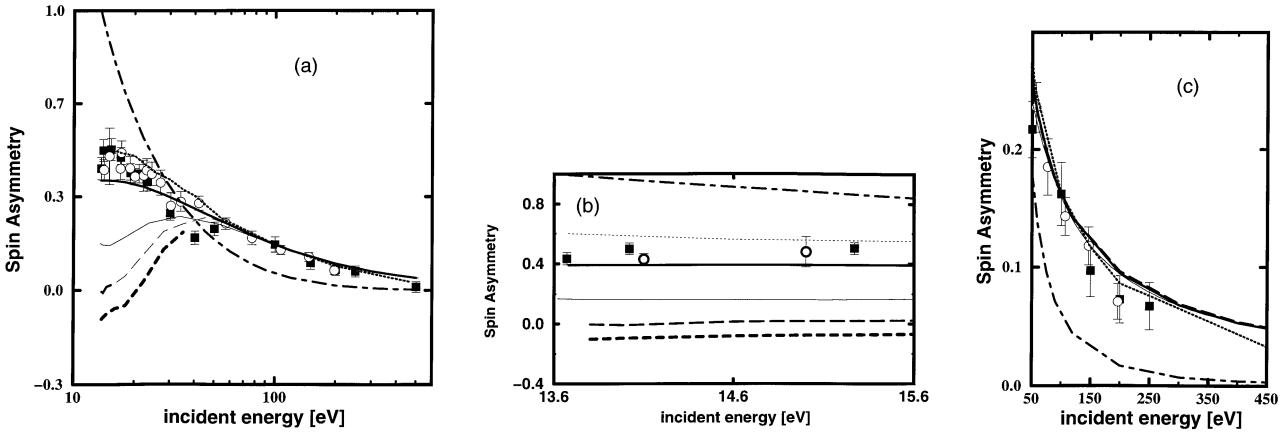

Fig. 3a–c. The spin asymmetry, as defined by (25), is shown for the ionization of atomic hydrogen by electron impact as function of the incident electron energy. **a** shows the results of the calculations using the 2C approximation (*solid curve*) whereas the *dotted curve* denotes the CCC results [20]. The *long-dashed curve* is the result of the FBA treatment whereas the PWIA leads to the spin asymmetry shown by the *dash-dotted curve*. The 3C (*short-dashed curve*) and the CDS2C (*light solid curve*) results are also depicted. The experimental data are due to [15] (*full squares*) and [14] (*open circles*). **b** the spin asymmetry is studied near to threshold. Curves are: *solid curve* (2C model), *short-dashed curve* (3C approximation), *long-dashed curve* (FBA), *light solid curve* (CDS2C model), *dotted curve* (Hidden crossing model [13]) and *dash-dotted curve* (PWIA results). Experimental data are as in **a**. **c** illustrates the high-energy behavior of A. Curves and data are the same as in **a**. Results of the 3C are not included

spin asymmetry. This shortcoming of the CDS2C and 3C approximation at lower excess energies is, as pointed out above, due to a spurious asymptotic behaviour of the modified Bessel function I_0 appearing in (19) which naturally results in a wrong threshold behaviour of the normalization N_{ab} and hence the erroneous spin-asymmetry predictions of the CDS2C and 3C models. This statement is re-enforced by the fact that the spin-asymmetry results in the CDS2C approximation are in better agreement with experiment than those due to the 3C treatment (Fig. 3a, b). Also included in Fig. 3a are the results of the convergent-close coupling method, CCC, [20]. The results of the CCC are in very good agreement with the experimental finding, however, close to threshold the evaluation of $\sigma(E)$ is limited by the computational resources as a rapidly increasing number of pseudo states is needed to achieve convergence. The results of the method using hidden-crossing theory [13] are also depicted in Fig. 3b. The variation shown by the latter calculations near threshold is at variance with the Wannier predictions of a constant value of A [18] and has been assigned to anharmonic corrections to the Wannier threshold law for triplet spin states. As expected, in the high energy region (Fig. 3c), triplet and singlet spin states are equally populated and hence $\lim_{1 \ll E} A \to 0$. In this case the behaviour of A is sufficiently well described by the CCC, CDS2C, 2C and FBA treatments which almost coincide with each other whereas the PWIA prediction of the spin asymmetry tend to the results of the other models at much higher energies.

Approximating the final-state wavefunction by the expression (6) means that the electron-electron final-state interaction is disregarded. This approximation becomes better for increasing nuclear charge in which case the electron-nucleus interactions dominates the electron-electron repulsion. For larger nuclear charge the Wannier threshold law (10) tends to a linear dependence, i.e. $\sigma(E) \propto E$, which is the threshold law predicted by the 2C model, as shown above. Thus, it is worthwhile to investigate the spin asymmetry A for increasing nuclear charge, i.e. for the electron-impact ionization of hydrogen-like ions. In this case the final-state is still described by the wavefunction (6). The initial state, given by (4), has however a different form and the calculations of $\sigma(E)$, as given by (1), become more elaborate and will be presented elsewhere. In the context of this work it is interesting to investigate the threshold behaviour of the spin asymmetry A with increasing nuclear field. First we remark that an analysis of the experimental spin-asymmetry data for ionization of atomic hydrogen has revealed a marginally positive slope of A at threshold [19]. This slightly positive slope of A develops into an identifyable peak in electron-lithium [16] and electron-sodium [16] impact ionization. The 2C-model calculations for a hydrogen-like positive ion, Fig. 4, clearly shows the emergence of a peak in the spin asymmetry for increased nuclear charge. This allows the interpretation of this peak, and indeed of the positive slope of A in the electron-hydrogen scattering, as being due to the electron-nucleus final-state interaction. Besides, the results of Fig. 4 and the experimental data of [16] lead to the interesting, however anticipated, conclusion that at low excess energy the main contribution to the measured spin asymmetry in electron lithium and sodium ionising collisions originates from small impact parameter scattering where the ionized electrons experience the net nuclear charge.

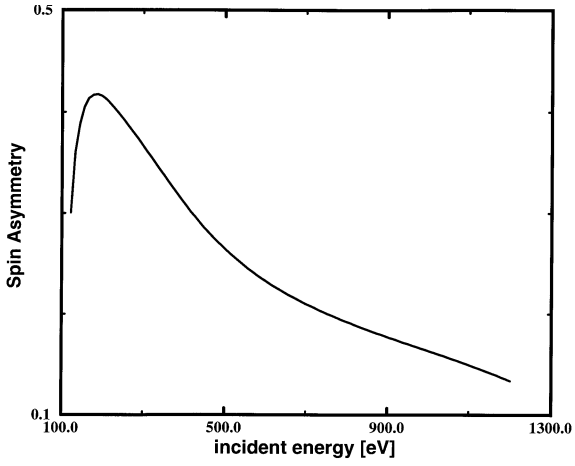

Fig. 4. The spin asymmetry, as defined by (25), for the ionization of Li^{++} by electron impact is depicted as a function of the incident energy. The binding energy of Li^{++} is 122.4 eV. For the calculations the 2C approximation (6) has been employed

IV Conclusions

In this work the integrated cross sections for the electron-impact ionization of atomic hydrogen has been investigated. The influence of individual final-state interactions on the structure of the spin-asymmetry as well as on the spin nonresolved total cross section and the energy-distribution between the escaping electrons have been analysed. It has been shown that when describing the two-electron continuum final-state within an independent Coulomb particle model, the shape of the spin non-resolved total cross sections as well as the energy-sharing between the escaping electrons and the spin asymmetry in the total cross section are in qualitative agreement with the Wannier-theory predictions. Furthermore, it has been shown that the measured analytical dependence and absolute value of the spin asymmetry is well reproduced by the independent Coulomb particle model over the entire measured energy region. To account for the final-state electronic correlations the 3C and the CDS2C models have been used. Although these two models can be successful in predicting near-threshold relative angular distributions of the emerging electrons, the results for the integrated cross sections investigated here are quite poor. This shortcoming has been traced back to a spurious threshold behavior of the radial part of the 3C wavefunction (8). Finally, by examining the spin asymmetry for hydrogen-like ions, it has been argued that the slightly positive slope observed in the spin asymmetry near threshold is due to the electron-nucleus final state interactions.

We would like to thank Michael Cremer, Jan-Michael Rost and John Briggs for many stimulating discussions. We also would like to thank Steve Buckman and Erich Weigold for helpful suggestions and comments. Financial support by the EU Human Capital and

Mobility Programme under contract No. CT930350 and the Alexander von Humboldt Foundation and the Australian National University is gratefully acknowledged.

References

1. Wannier, G.: Phys. Rev. **90**, 817 (1953)
2. Peterkop, R.K.: J. Phys. B. **4**, 513 (1971)
3. Cvejanović, S., Read, F.H.: J. Phys. **B7**, 1841 (1974)
4. Read, F.H.: Electron impact ionization, p. 42. Märk, T.D., Dunn, G.H. (eds.). New York, Berlin, Heidelberg: Springer 1984
5. Rau, A.R.P.: Phys. Rev. **A4**, 207 (1971)
6. Klar, H., Schlecht, W.: J. Phys. **B9**, 1699 (1976)
7. Klar, H.: J. Phys. **B14**, 3255 (1981)
8. Rau, A.R.P.: Phys. Rep. **110**, 369 (1984)
9. Feagin, J.M.: J. Phys. **B17**, 2433 (1984)
10. Kossmann, K., Schmidt, V., Andersen, T.: Phys. Rev. Lett. **60**, 1266 (1988)
11. Lablanquie, P., Ito, K., Morin, P., Nenner, I., Eland, J.H.D.: Z. Phys. D**16**, 77 (1990)
12. Rost, J.-M.: J. Phys. B**28**, 3003 (1985)
13. Macek, J.H., Ovchinnikov, S. Yu.: Phys. Rev. Lett. **74**, 4631 (1995)
14. Crowe, D.M., Guo, X.Q., Lubell, M.S., Slevin, J., Eminyan, M.: J. Phys. B**23**, L325 (1990)
15. Fletcher, G.D., Alguard, M.J., Gay, T.J., Hughes, V.W., Wainwright, P.F., Lubell, M.S., Raith, W.: Phys. Rev. A**31**, 2854 (1985)
16. Baum, G., Moede, M., Raith W., Schröder, W.: J. Phys. B**18**, 531 (1985)
17. Bartschat, K.: Phys. Rep. **180**, 1 (1989)
18. Greene, C.H., Rau, A.R.P.: Phys. Rev. Lett. **48**, 533 (1982)
19. Guo, X.Q., Crowe, D.M., Lubell, M.S., Tang, F.C., Vasilakis, A., Slevin, J., Eminyan, M.: Phys. Rev. Lett. **65**, 1857 (1990)
20. Bray, I., Stelbovics, A.T.: Phys. Rev. Lett. **70**, 746 (1993)
21. Botero, J., Macek, J.H.: Phys. Rev. Lett. **68**, 576 (1992)
22. Whelan, C.T., Allan, R.J., Rasch, J., Walters, H.R.J., Zhang, X., Röder, J., Jung, K., Ehrhardt H.: Phys. Rev. A**50**, 4394 (1994)
23. Röder, J., Rasch, J., Jung, K., Whelan, C.T., Ehrhardt, H., Allan, R.J., Walters, H.R.J.: Phys. Rev. A**53**, 225 (1995)
24. Garibotti, G., Miraglia, J.E.: Phys. Rev. A**21**, 572 (1980)
25. Brauner, M., Briggs, J.S., Klar, H.: J. Phys. B**22**, 2265 (1989)
26. Luke, Y.L.: Mathematical functions and their approximations. New York: Academic Press 1975
27. Abramowitz, M., Stegun, I.A. (eds.): Pocketbook of mathematical functions. Frankfurt: Harri Deutsch 1984
28. Berakdar, J.: Phys. Rev. A**53**, 2314 (1996)
29. Berakdar, J.: Aust. J. Phys. **49**, 1095 (1996)
30. Cremer, M.: Diploma thesis, University of Freiburg 1994
31. Berakdar, J.: (unpublished)
32. Cvejanović, S., Shiell, R.C., Reddish, T.J.: J. Phys. B**28**, L707 (1995)